Neutral copper(i) dipyrrin complexes and their use as sensitizers in dye-sensitized solar cells

Citation for published version:
Hewat, TE, Yellowlees, LJ & Robertson, N 2014, 'Neutral copper(i) dipyrrin complexes and their use as sensitizers in dye-sensitized solar cells' Dalton Transactions, vol. 43, no. 10, pp. 4127-4136. DOI: 10.1039/c3dt53334d

Digital Object Identifier (DOI):
10.1039/c3dt53334d

Link:
Link to publication record in Edinburgh Research Explorer

Document Version:
Peer reviewed version

Published In:
Dalton Transactions

Cite as:
Hewat, T. E., Yellowlees, L. J., & Robertson, N. (2014). Neutral copper(i) dipyrrin complexes and their use as sensitizers in dye-sensitized solar cells. *Dalton Transactions*, *43*(10), 4127-4136.

Manuscript received: 26/11/2013; Accepted: 19/01/2014; Article published: 24/01/2014

Neutral copper(I) dipyrrin complexes and their use as sensitizers in dye-sensitized solar cells**

Tracy E. Hewat,[1] Lesley J. Yellowlees[1] and Neil Robertson[1,*]

[1]EaStCHEM, School of Chemistry, Joseph Black Building, University of Edinburgh, West Mains Road, Edinburgh, EH9 3FJ, UK.

[*]Corresponding author; e-mail: neil.robertson@ed.ac.uk; fax: +44 (0)131 650 4743;
tel: +44 (0)131 650 4755

[**]We thank EPSRC (Supergen Excitonic Solar Cells) for financial support. We also thank the COSMIC facility at Edinburgh University for carrying out lifetime measurements. This work has made use of the resources provided by the EaStChem Research Computing Facility (http://www.eastchem.ac.uk/rcf). This facility is partially supported by the eDIKT initiative (http://www.edikt.org).

Graphical abstract:

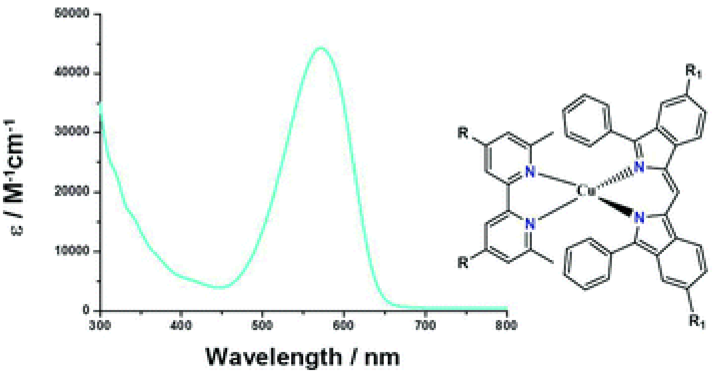

Heteroleptic neutral copper(I) dipyrrin complexes have been synthesised with the general formula [Cu(4,4'-(R)-6,6'-(CH_3)-bipyridine)(dipyrrin)], R = CH_3 or CO_2Et, and H-dipyrrin is either 1,3,7,9-tetramethyldipyrromethene (H**L1**), 1,13-diphenyl-6,8-diisoindolemethene (H**L2**), or 1,13-diphenyl-3,11-di(trifluoromethyl)-6,8-diisoindolemethene (H**L3**). Improved stability was observed across the series **L1** – **L3**, likely due to better steric constraints between the ligands. Visible light absorption has also been enhanced with a red-shift in absorption from 450 nm to 600 nm. Complex **3** shows photoluminescence lifetime in the order of nanoseconds suggesting singlet fluorescence which is supported by theoretical calculations. Study of the complexes as sensitisers in dye-sensitised solar cells was achieved by assembling the dye *in situ* on the surface of TiO_2 in a series of steps (anchoring ligand followed by ancillary ligand and $[Cu(CH_3CN)_4][BF_4]$. The highest efficiency achieved was 0.41 % for the dye with **HL3**, attributed to better dye regeneration due to a more favourable oxidation potential.

Introduction

Copper(I)-polypyridyl complexes have attracted a lot of recent interest as alternatives to Ru(II)-polypyridyls in photophysical and photoelectrochemical applications, particularly due to their ease of synthesis, their low toxicity, and the high abundance of copper in comparison with 2nd or 3rd row transition metals. This has led to use of such species in Organic Light Emitting Diodes (OLEDs),[1-3] light-emitting electrochemical cells (LECs) [4, 5] and Dye Sensitised Solar Cells (DSSCs).[6-18]

Copper(I)-polypyridyl complexes can display long-lived metal-to-ligand charge transfer (MLCT) excited states due to the d^{10} configuration, which avoids low-lying metal d-d states that might cause non-radiative decay. However, conformational change of the complex following MLCT excitation may lead to rapid non-radiative decay,[19, 20] and similarly, conformational change following Cu(I)/Cu(II) oxidation leads to slow electron transfer. To achieve Cu(I) complexes suitable for photoelectrochemical applications, this must be prevented by ligand design.[21] Typically addition of bulky substituents in the 6,6'-positions of bipyridine or 2,9-positions of phenanthroline will minimise the conformational change and maintain the pseudo-tetrahedral geometry. Another method is to have a large ancillary ligand to enhance steric rigidity.[6-9, 11, 20, 22.]

For solar energy applications, chromophoric ligands are attractive to enhance light harvesting. The BODIPY dye family has been widely studied as they are highly fluorescent; soluble in most organic solvents; they have a narrow emission bandwidth; are highly photostable; and have a relatively long-lived excited state.[23-25] This makes them ideal candidates in a wide range of applications such as biofluorescent probes, photosensitisers or pigments for dye lasers.[24-26]

In this context, dipyrromethene (hereafter dipyrrin) species, that form the delocalised framework of BODIPYs, have been used as ligands for a range of metals such as Pt(II),[27] Cu(II),[28] Ru(II),[29] Ir(III),[30] Zn(II)[26] and more recently Cu(I).[31] The unsubstituted parent compound is unstable,[32, 33] however stability is enhanced by adding groups at the *meso*-position and 1,9-positions to block nucleophillic or electrophillic attack.

Generally, dipyrrins have been used to form divalent or trivalent homoleptic complexes, with limited reports of heteroleptic species. A recent report described the first synthesis of heteroleptic Cu(I) dipyrrin complexes with phosphine ancillary ligands, and concluded that the low energy absorption and emission bands were intraligand charge transfer and thus the complex displayed fluorescence rather than phosphorescence.[31] Teets *et al* reported the first neutral Cu(I) complex of the related azadipyrromethene complex,[34] which was weakly luminescent at room temperature.

Given the emerging importance of Cu(I) polypyridyl complexes in optoelectronic fields, such species that also incorporate a dipyrrin ligand would form an attractive and tunable family of functional dyes. Accordingly, this work focuses on the synthesis and analysis of the first examples of copper(I) complexes that feature a dipyrrin ligand and a functionalised 2,2'-bipyridyl ligand. A first assessment is made of the potential of this complex type to be applied as sensitisers to dye-sensitised solar cells, in which context increased light harvesting, tunable redox potential and a long-lived charge-transfer excited state are all key features to optimise. We have used three different dipyrrin ligands (Fig. 1), with varying degrees of π-conjugation and substituents, to explore the effect on the photophysical and electrochemical properties of the dye. The bipyridine ligands used have substituents in 6,6'-positions to maintain a pseudo-tetrahedral geometry upon excitation. An *in-situ* dye assembly method on the TiO_2 surface was adopted to establish that such species can function as sensitisers.[12,13]

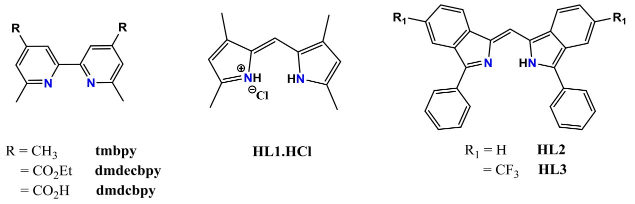

Fig.1 Ligands used in this work.

Experimental

General Procedures

The synthesis of $[Cu(CH_3CN)_4][BF_4]$,[35] 4,4'-6,6'-dimethyl-2,2'-bipyridine (tmbpy),[36] 4,4'-dicarboxy-6,6'-dimethyl-2,2'-bipyridine (dmdcbpy),[9, 37, 38] 1,3,7,9-tetramethyldipyrromethene (HL1.HCl),[39] and 1,13-diphenyl-6,8-diisoindolemethene (HL2),[40] were carried out according to literature procedures. 4,4'-(CO_2Et)-6,6'-dimethyl-2,2'-bipyridine (dmdecbpy) was synthesised by adapted literature procedures.[8] 1,13-diphenyl-3,11-di(trifluoromethyl)-6,8-diisoindolemethene (HL3) is a novel ligand adapted from literature methods for related species (see ESI† for procedure)[40-42] All other chemicals were purchased from

Sigma Aldrich, VWR, Fischer Scientific, Merck and used as received, except for 2,4-lutidine which was purified further by vacuum distillation.

All UV/Vis spectra were recorded using a JASCO V-670 series spectrophotometer and the data collected using Spectra Manager™ II software. Emission spectra were recorded at room temperature and 77 K in ethanol, using a Fluoromax2 fluorimeter controlled by the ISAMain software. Electrochemical studies were recorded using the General Purpose Electrochemical System (GPES) software that was connected to an Autolab system containing a PGSTAT 30. The technique comprised a Pt disk working electrode, a Pt rod counter electrode, and an Ag/AgCl reference electrode. The data collected were standardised against ferrocene/ferrocenium (measured at +0.507 V),[43] and adjusted for NHE (addition of 0.23 V to Ag/AgCl values). The supporting electrolyte was 0.1 M tetrabutylammonium tetrafluoroborate in acetonitrile.

Theoretical calculations were performed using the functional B3LYP, and the basis set LANL2DZ, to describe the copper atom and all other atoms were described by 6-31G*.[44-47] The initial structure was computed using Avogadro software[48] and frequency calculations were generated from the optimised geometry. Time-dependent density functional theory (TD-DFT) calculations were carried out using an acetonitrile polarisable continuum model and seventy singlet-singlet transitions were calculated using the optimised geometry.

Synthesis of Cu(L1)(tmbpy): (1)

[$Cu(CH_3CN)_4$][BF_4] (39.6 mg, 0.13 mmol), HL1.HCl (29.8 mg, 0.13 mmol) and 1M NaOH (0.25 mL) were added to degassed acetone (10 mL) and CH_2Cl_2 (5 mL). The solution was stirred at room temperature, under nitrogen, for 15 mins. Tmbpy (26.7 mg, 0.13 mmol) was added to the mixture and the solution was stirred for a further 45 mins. The mixture was filtered and the solvent was removed under reduced pressure. The resulting yellow/brown solid was stirred in water for 30 mins and then filtered. Yield: 46.2 mg, 77 %. ^{1}H NMR (DMSO, 400 MHz): δ 8.00 (s, 2H, H-bpy), 7.11 (s, 2H, H-bpy), 6.87 (s, 1H, CH-*meso*), 5.99 (s, 2H, H-pyrrolic), 2.50 (s, 6H, CH_3-bpy), 2.36 (s, 6H, CH_3-bpy), 2.28 (s, 6H, CH_3-L3), 2.18 (s, 6H, CH_3-L3). +ESI/MS: *m/z* 475.4 (M^+). Anal. Calc. for $C_{27}H_{31}CuN_4$: C 68.26, H 6.58, N 11.79. Found: C 68.19, H 6.53, N 11.64.

Synthesis of Cu(L2)(tmbpy): (2)

[$Cu(CH_3CN)_4$][BF_4] (28 mg, 0.09 mmol), HL2 (35 mg, 0.09 mmol) and 1M NaOH (0.09 mL) were added to degassed acetone (10 mL) and stirred at room temperature, under nitrogen, for 15 mins. Tmbpy (19 mg, 0.09 mmol) was added and the solution was stirred for a further 45 mins. The mixture was filtered and the solvent was removed under reduced pressure. The purple solid was washed with water and dried. Yield: 47.6 mg, 78.3 %. ^{1}H NMR (DMSO, 400 MHz): δ 8.30 (s, 1H, CH), 8.25 (d, 2H, J = 7.9 Hz, H-L4), 7.84 (s, 2H, H^5-bpy), 7.68 (d, 2H, J = 7.9 Hz, H-L4), 7.33 (t, 2H, J = 7.6 Hz, H-L4), 7.31 (d, 4H, J = 7.4 Hz, Ph), 7.13 (t, 2H, J = 7.4 Hz, H-L4), 6.96 (s, 2H, H^3-bpy), 6.89 (t, 2H, J = 7.3 Hz, Ph), 6.72 (t, 4H, J = 7.6 Hz, Ph), 2.31 (s, 6H, CH_3^6-bpy), 2.01 (s, 6H, CH_3^4-bpy). +ESI/MS: *m/z* 457.2 (CuL4). Anal. Calc. for $C_{43}H_{35}CuN_4$: C 76.93 H 5.26 N 8.35. Found C 76.82 H 5.20 N 8.26.

Synthesis Cu(L2)(dmdecbpy): (3)

[$Cu(CH_3CN)_4$][BF_4] (24 mg, 0.08 mmol), HL2 (30 mg, 0.08 mmol) and 1M NaOH (0.08 mL) were added to degassed acetone (10 mL) and stirred at room temperature, under nitrogen, for 10 mins. Dmdecbpy (25 mg, 0.08 mmol) was added to the solution and stirred for a further 1.5 h. The mixture was filtered and the solvent was removed under reduced pressure. The purple solid was washed with water and dried. A sephadex column (MeOH, then acetone) was used for further purification.Yield: 48.8 mg, 81.3 %. ^{1}H NMR (DMSO, 500 MHz): δ 8.35 (s, 2H, H^5-bpy), 8.34 (s, 1H, CH), 8.28 (d, 2H, H-L4), 7.66 (s, 2H, H^3-bpy), 7.64 (s, 2H, H-L4), 7.36 (t, 2H, H-L4), 7.20 (d, 4H, Ph), 7.15 (t, 2H, H-L4), 6.83 (t, 2H, Ph), 6.70 (t, 4H, Ph), 4.45 (q, 4H, O-CH_2), 2.18 (s, 6H, CH_3^6-bpy), 1.41 (t, 6H, CH_3). +ESI/MS: *m/z* 804 [M+NH_4]. Anal. Calc. for $C_{47}H_{39}CuN_4O_4$: C 71.69, H 4.99, N 7.12. Found: C 71.79, H 4.92, N 6.96.

Synthesis of Cu(L3)(tmbpy): (4)

[$Cu(CH_3CN)_4$][BF_4] (23 mg, 0.07 mmol), HL3 (40 mg, 0.07 mmol) and 1M NaOH (0.07 mL) were added to degassed acetone (10 mL) and stirred at room temperature, under nitrogen, for 15 mins. Tmbpy (16 mg, 0.07 mmol) was added and the solution was stirred for a further 1.5 hours. The mixture was filtered and the solvent was removed under reduced pressure. The purple solid was washed with water and dried. The solid was purified by washing with toluene to filter off the impurity ($Cu(tmbpy)_2BF_4$) and then running a Sephadex column in DMF to remove any further free ligands. Solvent was removed from the filtrate to yield the pure product. Yield: 15 mg, 25 %. ^{1}H NMR (DMSO, 500 MHz): δ 8.62 (s, 1H, CH), 8.53 (d, 2H, H-L4), 7.91 (s, 4H, H-L4), 7.84 (s, 2H, H^5-bpy), 7.63 (d, 2H, H-L4), 7.22 (d, 4H, Ph), 6.99 (s, 2H, H^3-bpy), 6.96 (t, 2H, Ph), 6.77 (t, 4H, Ph), 2.36 (s, 6H, CH_3^6-bpy), 1.99 (s, 6H, CH_3^6-bpy). ^{19}F NMR (DMSO, 376 MHz): δ -59.17, -59.41.

Synthesis of Cu(L3)(dmdecbpy): (5)

[$Cu(CH_3CN)_4$][BF_4] (20 mg, 0.07 mmol), HL3 (35 mg, 0.07 mmol) and 1M NaOH (0.07 mL) were added to degassed acetone (10 mL) and stirred at room temperature, under nitrogen, for 15 mins. Dmdecbpy (21 mg, 0.07 mmol) was added and the solution was stirred for a further 1.5 hours. The mixture was filtered and the solvent was removed under reduced pressure. The purple solid was washed with water and dried. The solid was purified by washing with toluene to filter off the impurity ($Cu(dmdecbpy)_2BF_4$) and then running a Sephadex column in DMF to remove any further free ligands, but some free ligands still remained. Yield: 6 mg, 10 %. ^{1}H NMR (DMSO, 500 MHz): δ 8.67 (s, 1H, CH), 8.63 (s, 2H, H^5-bpy), 8.56 (d, 2H, H-L4), 7.89 (s, 2H, H-L4), 7.81 (s, 2H, H^3-bpy), 7.66 (d, 2H, H-L4), 7.22 (d, 4H, Ph), 6.89 (t, 2H, Ph), 6.75 (t, 4H, Ph), 4.41 (q, 4H, O-CH_2), 2.69 (s, 6H, CH_3^{6}-bpy), 1.37 (t, 6H, CH_3). ^{19}F NMR (DMSO, 376 MHz): δ -59.26, -59.51.

Preparation of solar cells

Titanium dioxide paste (Dyesol, DSL-18NR-T) was deposited onto pre-treated ($TiCl_4$, 40 mM, 75 °C for 30 mins) fluorine-doped tin oxide conductive glass (3 mm thick, 8 Ω sheet resistance, Solaronix) by doctor-blading. The film thickness was approx 11 μm. The TiO_2 electrodes (active area = 4x4 mm^2) were heated to 500 °C for 30 min, cooled to room temperature, treated with a dilute solution of $TiCl_4$ (40 mM, 75 °C for 30 mins) and sintered at 500 °C for 30 min. The electrodes were allowed to cool (80-100 °C) and immersed into a DMSO solution of **dmdcbpy** (3 mM) overnight. The colourless slide was removed from the solution and washed with DMSO followed by ethanol and dried. The electrodes were then immersed into a acetonitrile solution of $[Cu(CH_3CN)_4][BF_4]$ (1 mM) and **HL1.HCl**, **HL2**, or **HL3** (1 mM) for 24 h. The electrodes were removed and washed with acetonitrile and dried. Counter electrodes were platinized using 10 μL of H_2PtCl_6 solution (5 mM) in isopropyl alcohol and heated to 400 °C for 15 minutes. The solar cells were assembled by sandwiching the two electrodes together using a sealant (Bynel, 25 μm), and heated to 220 °C, applying even pressure to ensure the Bynel melted evenly. Electrolyte was vacuum filled into the hole and the hole was sealed by Bynel and a cover glass. Current-voltage behaviour of the cells was determined using a Sciencetech solar simulator equipped with an AM 1.5G filter, calibrated to 100 $mWcm^{-1}$ using a silicon photodiode. The electrolyte used was 0.4 M lithium iodide (LiI), 0.03 M iodine (I_2), 0.1 M guanidinium thiocyanate (GuNCS), 0.5 M *tert*-butylpyridine (TBP), 1 M 1,3-dimethylimidazolium iodide (DMII) in acetonitrile:valeronitrile (MeCN:VN) 85:15.

Results and Discussion

Syntheses

Copper(I) dipyrrin complexes were synthesised at room temperature via a simple one-pot method (Fig. 2) using stoichiometric quantities of ligands and base (to deprotonate the free dipyrrin ligand). The reaction was carried out under nitrogen to minimise oxidation to copper(II). Further purification was achieved by Sephadex column where necessary (**3** – **5**). The complexes were characterised by ^{1}H NMR, ESI-MS and elemental analysis, confirming the proposed structures. In the case of **4** and **5**, only NMR characterisation was possible due to difficulties in obtaining sufficient yield (**4**) and residual ligand impurities (**5**). Clearly, complex formation with the new ligand **L3** has proven difficult, however we include **4** and **5** in the study as they have the greatest relevance to DSSC application and the *in situ* dye assembly described later.

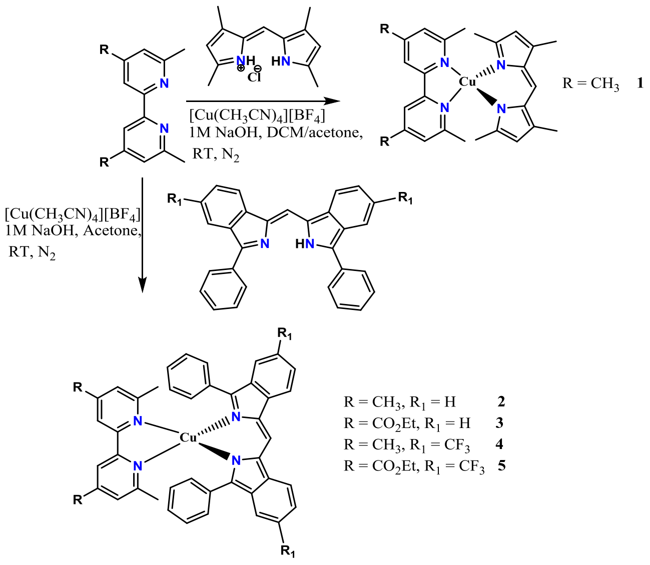

Fig.2 Reaction scheme of neutral copper(I) complexes.

Stability and reproducibility

Copper(I) complexes are extremely labile which accounts for the common reproducibility problems for heteroleptic species. [12, 49, 50] During the reaction, ligands will continually exchange with other ligands in solution, giving rise to a mixture of products, unless one is more favoured due to steric constraints or binding energies.

The stability of complexes **1-3** in solution was explored via ^{1}H NMR at varying time intervals; 0, 7 and 17 days. The stability of **2** is shown in Fig.3.

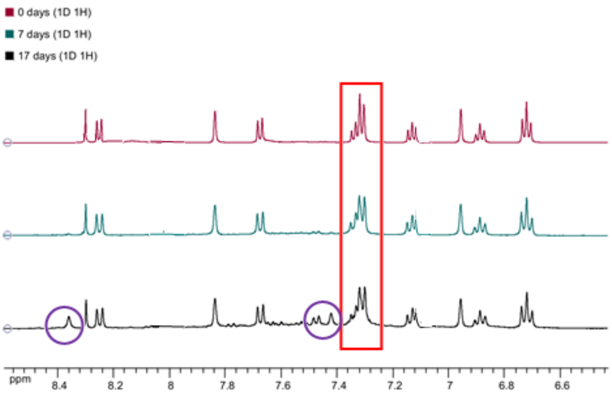

Fig.3 Stability testing of **2** in d_6-DMSO by NMR.

After seven days, there is a slight change in the intensity of the peak at 7.31 ppm, representing the phenyl group on the dipyrrin ligand (red box), which became more noticeably different after 17 days. After 17 days there are also new peaks (purple circles) arising which suggests $[Cu(tmbpy)_2][BF_4]$ (8.36 ppm and 7.42 ppm) is forming in solution with the breakdown of the complex. The long-term instability in solution is the likely reason that precluded the growth of single crystals for diffraction. This is similarly observed for complexes **1** and **3** (ESI†).

UV-Vis Absorption Spectroscopy

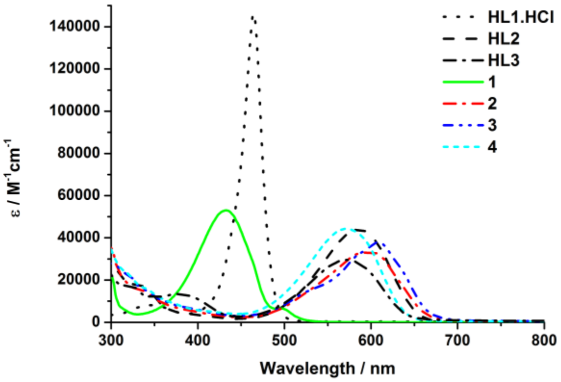

Fig. 4 Absorption spectra of ligands (**HL1.HCl**, **HL2** and **HL3**) and complexes (**1-4**) in acetonitrile.

The spectra of all ligands and complexes display the characteristic intense visible absorption typical of dipyrrins. The noticeable difference between the protonated ligand (**HL1.HCl**) and complex **1** is the considerable decrease in intensity and broadening of the main band (432 nm) when the dipyrrin is coordinated to copper. Within porphyrin chemistry this is usually a result of loss in degeneracy of the LUMO[51] and a similar effect may be occurring here. Complex **1** also shows a second absorption at longer wavelengths (498 nm).

Increasing the conjugation of the dipyrrin backbone for **HL2** results in a red shift of the π-π* transition from 464 nm (**HL1.HCl**) to 584 nm, and a decrease in the intensity and broadening of the band, possibly due to phenyl rotation. Generally, increasing conjugation will reduce the HOMO-LUMO gap of the ligand hence lower the energy of the π-π* transition. Adding electron-withdrawing groups (CF_3) to the dipyrrin (**HL3**) resulted in a slight blue shift in comparison to **HL2**.

Complexes **2** and **3** show very similar spectroscopic properties, with the main visible band around 600 nm, a slight red-shift from the free ligand. A slight red-shift and intensity difference between **2** and **3** is due to a change in substituents on bipyridine. Theoretically, increasing the electron-withdrawing character (methyl to an ester) will shift the MLCT absorption band to lower energies, and can also enhance the charge transfer character of the low-energy transitions where these involve orbitals on the bipyridine ligand. Complex **4** shows similar absorption values to **HL3** (570 nm), although the intensity is greater.

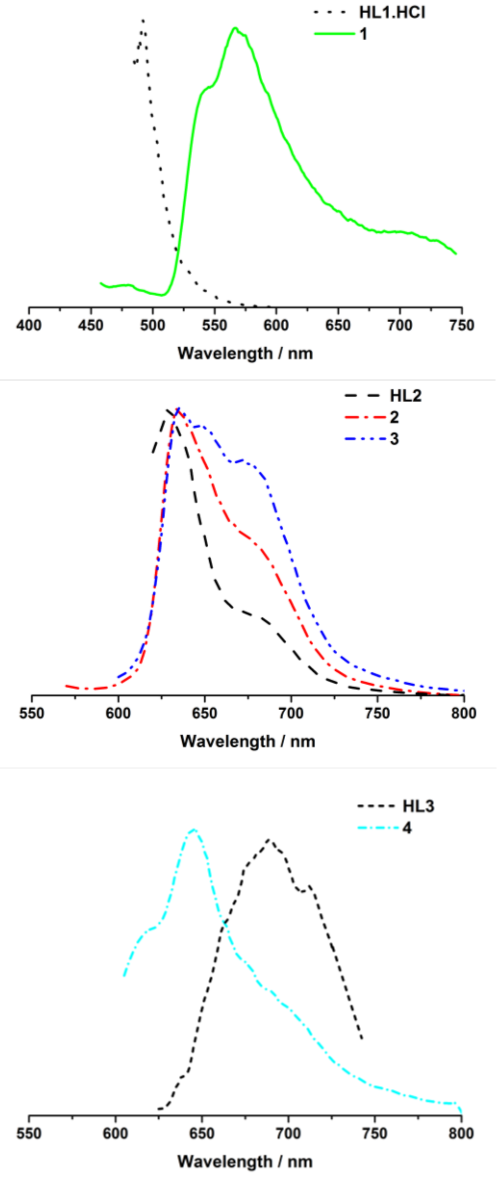

Fig. 5 Photoluminescence of (top) **HL1.HCl** and **1**, (centre) **HL2, 2** and **3** in Ethanol at 77 K (complex **1** recorded at room temperature) and (bottom) **HL3** and **4** in acetonitrile at 77 K.

Table 1 Photophysical properties of the ligands **HL1.HCl, HL2, HL3** and complexes **1-4**.

Compound	λ_{abs}^{a} / nm (ε_{max} (x10^3 $M^{-1}cm^{-1}$)	Room temperature ^{b}		77 K ^{b}		$<\tau>$ / ns ^{b}
		λ_{max}/nm Excitation	λ_{max}/nm Emission	λ_{max}/nm Excitation	λ_{max}/nm Emission	
HL1.HCl	464 (145)	485	492	470	490	Not recorded
HL2	584 (44.5)	600	650	605	630	0.25
HL3	571 (29.6)	590	650	580	660	Not recorded
1	432 (53.2) 498 (6.4)	390	490	370	490	Not recorded
2	600 (33.2)	530	665	550	635	Not recorded
3	608 (38)	540	665	560	640	0.34
4	572 (44.2)	570	645	585^{a}	645^{a}	Not recorded

^{a} measured in acetonitrile

^{b} measured in ethanol

Photoluminescence

Complexes **1-4** are emissive in ethanol at room temperature and 77 K. The results are summarised in Table 1 and compared with data for the free dipyrrin ligands. All of the complexes emit at a comparable energy to their respective free dipyrrin ligands and at room temperature, the emission maxima and the shape of the band for complexes **2**, **3** and **HL3** are all very similar. These observations suggest that the copper or bipyridine orbitals are not significantly involved in the transition. This is often seen in literature for dipyrrin complexes, or other highly chromophoric, conjugated ligands,[31, 52] where the photophysical behaviour derives solely from the ligand orbitals. The excitation data for complex **4** correlate well with the absorption and are very similar to the uncomplexed ligand **HL3**, which further supports the conclusion that the emissive behaviour derives from the dipyrrin. Complexes **1** – **3** show λ_{max} (excitation) values at higher energy than the maxima in their respective absorption spectra. Complexes **2** and **3** both display higher-energy emission when frozen, suggesting a significant degree of structural relaxation of the molecule after excitation that is prevented in the rigid matrix (77 K). In addition to this, the change in solvent (ethanol, acetonitrile and DCM) does not have a significant effect on the position and shape of the absorption and emission spectra, only in the intensity (ESI†). This implies that there is weak polarisation between the ground and excited states, supporting the assignment of the transition as ligand centred rather than charge transfer.[40]

Time-resolved fluorescence was used to measure the lifetime of complex **3** and ligand **HL2**, selected as representative samples that gave sufficient signal with the excitation laser wavelength available (shortest = 486 nm). The average excited-state lifetime observed for **HL2** and **3** are similar, with that of the complex being slightly longer. In keeping with the steady-state measurements, this similarity and also the nanosecond timescale, suggest that emission can be assigned as $^{1}(\pi\text{-}\pi^{*})$ fluorescence from the dipyrrin centre and not ^{1}MLCT or ^{3}MLCT. Dipyrrin centred intraligand charge transition was also reported in literature for copper(I) complexes with phosphine coligands.[31]

Electrochemistry

Table 2 Electrochemical data for ligands **HL1.HCl**, **HL2, HL3** and complexes **1-5** in 0.1 M TBABF$_4$ / MeCN *vs.* NHE.

Compound	E_{ox} / V	E_{red} / V
HClL1	1.55^{a}, 1.68	-0.45^{a}
HL2	0.84^{b}, 1.02^{b}	-
HL3	0.97^{b}, 1.08^{b}	-
1	0.97^{a}, 1.25	-1.44^{a}
2	0.45^{a}, 0.64^{b}, 0.86	-1.26^{a}
3	0.55^{a}, 0.68^{b}, 0.90	-1.18^{a}
4	0.62^{a}, 0.96^{b}, 1.12^{b}	In solvent window
5	0.76^{b}, 0.97, 1.13^{b}	-1.24^{a}

^{a} Irreversible

^{b} Pseudo-reversible

The redox potentials for free ligands and complexes are summarised in Table 2. Although the poor purity of **5** prevented its inclusion in the spectroscopic study, it has been included here since minor impurity peaks in the electrochemical data can be readily identified and neglected.

The reduction potentials reported for each complex can be assigned as bipyridine ligand based, although possibly also with some dipyrrin character in the case of **1** as suggested by computational work (*vide infra*). Complex **2** and complex **3** both display a similar oxidation potential attributed to the Cu(dipyrrin) fragment which remains unchanged between them. The irreversible character of these precludes interpretation of the subsequent oxidation processes. In the context of DSSC applications, these complexes show insufficiently positive oxidation potential to be used with the common redox electrolyte I^{-}/I_3^{-} [53] as the dye would not be rapidly regenerated.

Complex **1** is not as easily oxidised as **2** and **3**. The reason for this is due to less conjugation of the dipyrrin structure, also reflected in comparing **HL1**.HCl and **HL2**. This supports the assignment of the first oxidation for **2** and **3** as dipyrrin based, consistent with the electronic spectroscopy results, where the lowest excitation is localised on the dipyrrin.

Table 3 Percentage contributions from component parts of **1-3** to selected molecular orbitals. Also quoted are the calculated energies for these molecular orbitals.

Complex	MO	MO energy / eV	% Contribution from Cu-based orbitals	Dipyrrin-based orbitals	Bipy-based orbitals
1	HOMO-1	-4.80	66.58	13.32	20.1
	HOMO	-4.72	68.18	20.82	11.0
	LUMO	-1.94	3.26	2.19	94.55
	LUMO+1	-1.79	1.49	97.52	0.99
2	HOMO	-4.73	0.16	99.64	0.20
	LUMO	-2.24	2.30	96.0	1.70
	LUMO+1	-1.95	2.49	3.41	94.10
3	HOMO-3	-5.98	76.61	13.95	9.44
	HOMO-1	-5.19	63.58	19.17	17.25
	HOMO	-4.78	0.12	99.70	0.18
	LUMO	-2.74	4.99	5.73	89.28
	LUMO+1	-2.31	2.06	95.82	2.12
	LUMO+2	-2.29	0.53	3.60	95.87

Generally the redox processes for copper(I) complexes are not chemically reversible as observed here.[54]

Increasing the conjugation of the dipyrrin ligand red shifts the absorption, improving light harvesting. However, the complex becomes too easily oxidised. One method to resolve this is to add electron-withdrawing groups to dipyrrin structure, such as CF_3, CN, or NO_2 groups. This was the strategy behind the synthesis of **HL3**, **4** and **5** and indeed we observed a shift in oxidation potentials to more positive values.

Computational and Electronic Properties of Molecules

The experimental and calculated UV-Vis spectra for **1-3** are shown in Fig. 6. The calculated results are qualitatively comparable to experimental data, although with some differences in the exact energy of the visible transitions. For **1**, the lowest energy transition calculated at 581 nm represents MLCT from copper centre to either bipy or dipyrrin ligand, which is typical for heteroleptic copper(I) complexes.[33] The LUMO and subsequent levels are localised on dipyrrin and bipy as both ligands show similar electron-donating and withdrawing abilities and therefore one is not predominantly favoured over the other. Notably, the HOMO of **1** is calculated to have dominant Cu character in contrast to **2** and **3** where the HOMO is calculated to be almost entirely dipyrrin based. The dominant absorption feature in the visible spectrum, calculated at 399 nm, is shown to be predominantly ligand-centred on dipyrrin.

Complex **2**, which features the same bipyridine moiety as **1**, but more conjugated dipyrrin, showed a similar LUMO. The minimal electron-withdrawing functionality on the bipyridine positions these orbitals higher in energy such that the LUMO is localised on dipyrrin whereas the LUMO+1 is localised on bipy. TD-DFT data suggest the low-energy visible transition has a high contribution of ligand-centred character instead of charge transfer, suggesting that the metal centre does not significantly affect the absorption properties of the complex. This supports experimental data such as fluorescence with a short lifetime instead of phosphorescence and the ease of oxidation compared with **1**.

For **3**, the main visible absorption band shows a high contribution of copper-to-bipy (MLCT) transition and a small contribution localised on dipyrrin ligand (27%). A weak MLCT band is predicted at 744 nm, however with very low oscillator strength such that this band not observed in the experimental data. Table 3 indicates that the LUMO is now localised on the bipyridine ligand and the LUMO+1 is localised on the dipyrrin instead of the other way around for complex **2**. This is due to electron-withdrawing ester groups on bipyridine.

Table 4 TD-DFT calculated visible absorption wavelengths for **1-3**, illustrating the molecular orbitals involved and their relative contribution to the absorption.

Complex	Main visible absorbance / nm	Main charge transitions MO from	MO to	Relative Contribution (%)
1	581	HOMO-1	LUMO	23
		HOMO-1	LUMO+1	36
		HOMO	LUMO	41
2	541	HOMO	LUMO	66
		HOMO	LUMO+1	34
3	546	HOMO-3	LUMO	13
		HOMO-1	LUMO+2	60
		HOMO	LUMO+1	27

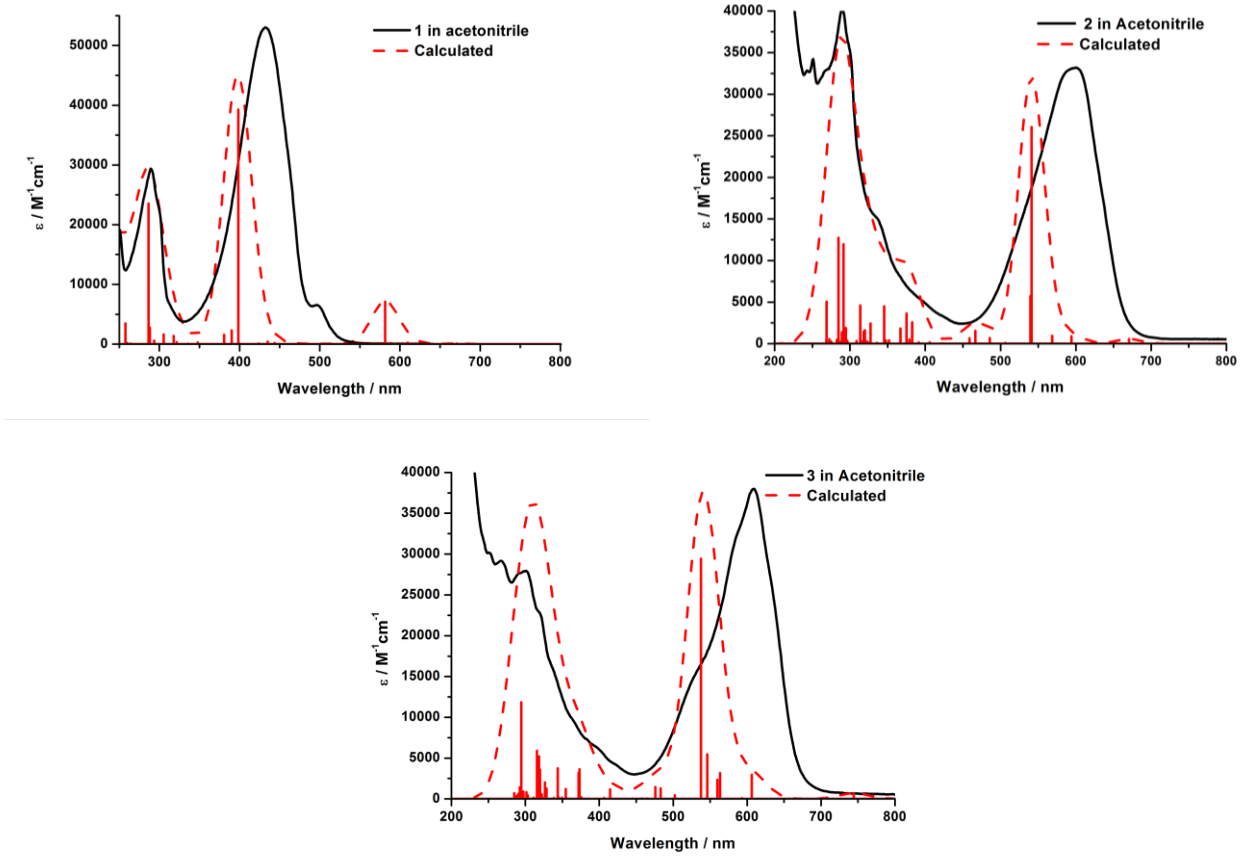

Fig.6 Theoretical UV-Vis spectra for **1-3**. Black line represents the experimental spectrum in acetonitrile, red dotted line represents the calculated spectrum, and red solid line represents the calculated electronic transition.

In-situ Solar Studies

The above studies included bipy ligands with carboxylic ester groups as these give information on the spectroscopic and electrochemical properties of dyes (**3** and **5**) appropriate for use as DSSC sensitisers. For solar cell fabrication however, dyes with acid, rather than ester functionality, are required and we experienced synthetic difficulty in the isolation of heteroleptic complexes consisting of an acid-bipy and dipyrrin ligand, due to the ease of deprotonation and reprotonation of dipyrrin. *In-situ* methods, based on the procedure of the Constable group,[12, 13] were therefore adopted to enable solar cell performance of these dyes to be assessed without the need to isolate the acid complexes.

The electrochemical properties indicate that **3** is too easily oxidised, such that it is poorly designed for use in DSSC with the I^-/I_3^- electrolyte. Complex **4** was designed to contain additional electron-withdrawing groups (CF_3) which results in a 0.07 V shift in oxidation potential to more positive values and **5** shows a further 0.14 V shift in oxidation potential. This suggests dye regeneration may be possible if the copper sensitiser features a dipyrrin with CF_3 groups. The method is shown in Fig. 7. Table 5 reports the efficiency data of the best cells.

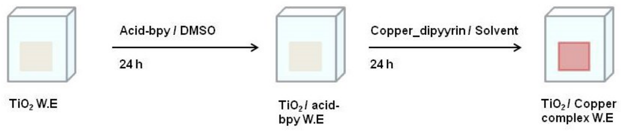

Fig.7 *In-situ* protocol for producing a copper complex on the surface of TiO_2 working electrode.

The working electrodes were first immersed into a DMSO solution of dmdcbpy ligand for 24 hours. The electrodes were rinsed and dried and then immersed into a solution of $[Cu(CH_3CN)_4][BF_4]$ and dipyrrin for 24 hours. The colour change is indicative of coordination occurring on the surface of TiO_2. For comparison, a reference cell was also prepared using the known homoleptic copper(I) dye (Fig. 8).[8]

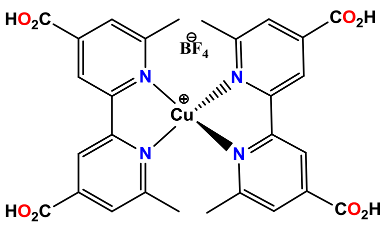

Fig.8 Homoleptic Cu(I) complex $[Cu(dmdcbpy)_2][BF_4]$.[8]

The electrolyte used in this work consisted of 0.4 M LiI, 0.03 M I_2, 0.1 M GuNCS, 0.5 M TBP, 1 M DMII in acetonitrile:valeronitrile (85:15).

The solar cell construction was explored (ESI†) via changes in (i) the solvent system, (ii) introducing either a [Cu(II)(dipyrrin)$_2$] homoleptic dye or Cu(I) salt as the copper source, and (iii) addition of base to deprotonate the dipyrrin prior to coordination. Changes in solvent system can affect the overall efficiency of the solar cell. For instance, dichloromethane or acetonitrile were used to dissolve the copper salt and dipyrrin. If dichloromethane were used in the dye bath the photocurrent was lower and the photovoltage was higher than if acetonitrile were used. This could suggest the energy of the acceptor states in the TiO$_2$ is higher for the DCM cell, affecting charge injection and reducing the photocurrent of the cell.

One method adopted to instigate ligand exchange whilst in solution used a homoleptic [Cu(II)(dipyrrin)$_2$] species. Several attempts were made to reduce the copper *in-situ*; Zn/Hg, NaBH$_4$ or methanol as the reducing agent. The most successful attempt used methanol. The colour change on the surface was either deep red or deep yellow, which is indicative of surface bound dye. However, the photocurrent voltage results were lower than using a copper(I) species as the starting reagent.

The following table represents the highest efficiencies achieved in this work. Sample **a** used the addition of [Cu(CH$_3$CN)$_4$][BF$_4$] and **HL1**.HCl to the bound acid-bipy anode in dichloromethane, **b** used the addition of [Cu(CH$_3$CN)$_4$][BF$_4$] and **HL2** in acetonitrile, and **c** used the addition of [Cu(CH$_3$CN)$_4$][BF$_4$] and **HL3** in acetonitrile.

Table 5 DSSC efficiency data of the best cells. The active layer was 0.16 cm^2 and the cells were measured under 1 sun.

Sample	V_{oc} / mV	J_{sc} / mAcm^{-2}	ff	η / %
[Cu(dmdcbpy)$_2$][BF$_4$]	530	2.33	0.68	0.83
a	520	0.40	0.62	0.13
b	510	0.91	0.68	0.31
c	520	1.21	0.64	0.41

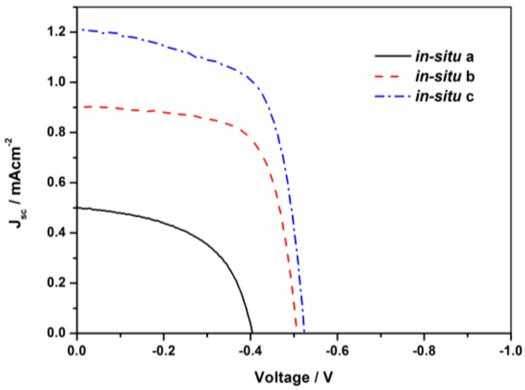

Fig.9 Photocurrent voltage curves of *in-situ* studies. The cells were all tested under the same conditions and the best cells are reported.

The charge injection should not greatly change between samples **a**, **b**, and **c** as the LUMO should be localised on the acid-bipy ligand. The improved photocurrent could be a result of improved dye regeneration which would be expected for **L3**; addition of electron-withdrawing groups (CF$_3$) to the dipyrrin ligand should reduce the HOMO energy level, causing the complex to be less easily oxidised and therefore improve dye regeneration. Sample **c** has indeed shown an increase in the cell's efficiency in comparison to samples **a** and **b**, through both an improved photocurrent and open-circuit voltage.

Conclusions

This work demonstrates the first examples of heteroleptic copper(I) complexes, consisting of a bipyridine ligand and a dipyrrin ligand. A series of three dyes has been synthesised and fully characterised by electrochemical, photophysical and computational techniques, with two other complexes obtained but difficult to fully study due to poor stability and low yield. Copper(I) materials are highly labile towards ligand exchange which inevitably poses problems with stability, especially when they are in solution for long periods of time. Interestingly, the complexes did show improved stability with enhanced steric constraint caused by the bulkiness of the dipyrrin ligand.

Increasing the π-conjugation of the dipyrrin ligand shifts the visible bands to lower energies. Complex **1** also shows a small band at 498 nm corresponding to MLCT transition, according to theoretical calculations. Complex **2** and **3** showed very similar absorption properties to the free dipyrrin ligand. Lifetime measurements suggest that complex **3** shows fluorescence rather than phosphorescence, with a nanosecond timescale.

According to electrochemical data, complex **2** and **3** are easily oxidised, which may cause a problem for dye regeneration within a DSSC device. Decreasing the conjugation (complex **1**) resulted in an increase in HOMO-LUMO gap, which ultimately blue-shifts the charge transfer transition and reduces light harvesting. Complex **4** features CF$_3$ groups which shift the oxidation potential to more positive values.

Despite the low oxidation potentials *in-situ* solar studies did show that the complexes assembled function as sensitisers, with efficiencies of 0.13 - 0.41%. The study shows that increasing the conjugation of dipyrrin ligand (**L1** to **L2**) improved the efficiency. It is likely that this is due to better light harvesting. The highest efficiency was obtained for the copper complex with **L3** ligand. The electron-withdrawing trifluoromethyl groups increased the oxidation potential, which possibly improved dye regeneration. Although the absolute value of these efficiencies remains low, we have demonstrated the concept of using a chromophoric ancilliary ligand on a heteroletic Cu(I) complex to enhance light harvesting. We hope this will stimulate further molecular design in the active field of DSSC sensitisers based on earth-abundant elements.[18]

Notes and references

School of Chemistry and EaStChem, University of Edinburgh, King's Buildings, Edinburgh, UK. E-mail: neil.robertson@ed.ac.uk; Fax: +44 131 650 4743; Tel: +44 131 650 4755

†Electronic Supplementary Information (ESI) available: Synthetic procedures for the synthesis of **HL3** and **dmdecbpy**; Figure S1: Reaction scheme for **HL3**; Figure S2: Stability tests of **1**; Figure S3: Stability tests of **3**; Figure S4: 2D COSY and 2D NOESY spectra of **3**; Figure S5: ^{19}F NMR of **HL3**; Figure S6: ^{1}H NMR spectra of **HL3** and **5**; Figure S7: (a) Absorbance spectrum of **HL2** in varying solvents, (b) Absorbance spectrum of **3** in varying solvents; Figure S8: Excitation and emission

spectra of **1-4**; Figure S9: Molecular orbital images of **1**; Figure S10: Molecular orbital images of **2**; Figure S11: Molecular orbital images of **3**; Figure S12: Differential pulse voltammograms of **1** – **5**; Table S1: Percentage contributions from component parts of **1** to selected molecular orbitals; Table S2: TD-DFT calculated visible absorption wavelengths of **1**; Table S3: Percentage contributions from component parts of **2** to selected molecular orbitals; Table S4: TD-DFT calculated visible absorption wavelengths of **2**; Table S5: Percentage contributions from component parts of **3** to selected molecular orbitals; Table S6: TD-DFT calculated visible absorption wavelengths of **3**; Table S7: Reagents and solvents used for *in-situ* solar studies; Table S8: JV data for *in-situ* solar studies. For ESI see DOI: 10.1039/b000000x/

1 Z. Liu, M. F. Qayyum, C. Wu, M. Whited, P. I. Djurovich, K. O. Hodqson, B. Hedman, E. I. Solomon, M. E. Thompson, *J. Am. Chem. Soc.,* 2011, **133**, 3700-3703.

2 I. Satoshi, H. Masashi, K. Isao, Y. Masataka, H. Mikio, O. Masahisa, *J. Mater. Chem. C.,* 2013, **1**, 542-551.

3 H. Masashi, I. Satoshi, Y. Masataka, K. Isao, H. Mikio, O. Masahisa, *J. Am. Chem. Soc.,* 2011, **133**, 10348-10351.

4 R. D. Costa, D. Tordera, E. Ortí, H. J. Bolink, J. Schönle, S. Graber, C. E. Housecroft, E. C. Constable, J. A. Zampese, *J. Mater. Chem.*, 2011, **21**, 16108-16118.

5 Y-M. Wang, F. Teng,Y-B. Hou, Z. Xu, Y.-S. Wang, *Appl. Phys. Lett.*, 2005, **87**, 233512-233515.

6 Alonso-Vante, J.-F. Nierengarten, J.-P. Sauvage, *J. Chem. Soc. Dalton Trans.*, 1994, 1649-1654.

7 S. Sakaki, T. Kuroki, T. Hamada, *J. Chem. Soc.*, *Dalton Trans.*, 2002, 840-842.

8 T. Bessho, E. C. Constable, M. Graetzel, A. H.Redondo, C. E. Housecroft, W. Kylberg, Md. K. Nazeeruddin, M. Neuburger, S. Schaffner, *Chem. Comm.*, 2008, 3717-3719.

9 E. C. Constable, A.H. Redondo, C. E. Housecroft, M. Neuburger, S. Schaffner, *Dalton Trans.*, 2009, 6634-6644.

10 B. Bozic-Weber, E. C. Constable, C. E. Housecroft, M. Neuburger, J. R. Price, *Dalton Trans.*, 2010, **39**, 3585-3594.

11 C. L. Linfoot, P. Richardson, T. E. Hewat, O. Moudam, M. M. Forde, A. Collins, F. White, N. Robertson, *Dalton Trans.*, 2010, **39**, 8945-8956.

12 B. Bozic-Weber, E. C. Constable, C. E. Housecroft, P. Kopecky, M. Neuburger, J. A. Zampese, *Dalton Trans.*, 2011, **40**, 12584-12594.

13 B. Bozic-Weber, V. Chaurin, E. C. Constable, C. E. Housecroft, M.Meuwly, M. Neuburger, J. A. Rudd, E.Schönhofer, L. Siegfried, *Dalton Trans.*, 2012, **41**, 14157-14169.

14 Y-J. Yuan, Z-T. Yu, J-Y. Zhang, Z-G. Zou, *Dalton Trans.*, 2012, **41**, 9594-9597.

15 B. Bozic-Weber, S. Y. Brauchli, E. C. Constable, S. O. Fürer, C. E. Housecroft, F. J. Malzner, I. A. Wright, J. A. Zampese, *Dalton Trans.*, 2013, **42**, 12293

16 N. Robertson, *Chem. Sus. Chem.*, **2008**, 977

17 M. Sandroni, M. Kayanuma, A. Planchat, N. Szuwarski,E. Blart, Y. Pellegrin, C. Daniel, M. Boujtita, F. Odobel, *Dalton Trans*., 2013, **42**, 10818

18 B. Bozic-Weber, E. C. Constable, C. E. Housecroft, *Coord. Chem. Rev.,* 2013, **257**, 3089

19 D. V. Scaltrito, D. W. Thompson, J. A. O'Callaghan, G. J. Meyer, *Coord. Chem. Rev.*, 2000, **208**, 243-266.

20 N. Amaroli, *Chem. Soc. Rev.*, 2001, **30**, 113-119.

21 R. M. Williams, L. De Cola, F. Hartl, J-J. Lagref, J-M. Planeix, A. De Cian, M. W. Hosseini, *Coord. Chem. Rev.*, 2002, **230**, 253-261.

22 N. Armaroli, G. Accorsi, F. Cardinali and A. Listorti, *Photochemistry and Photophysics of Coordination Compounds I*, 69, Springer, 2007.

23 R. Sakamoto, S. Kusaka, Y. Kitagawa, M. Kishida, M. Hayashi, Y. Takara, M. Tsuchiya, J. Kakinuma, T. Takeda, K. Hirata, T. Ogino, K. Kawahara, T. Yagi, S. Ikehira, T. Nakamura, M. Isomura, M. Toyama, S. Ichikawa, M. Okumura, H. Nishihara, *Dalton Trans.*, 2012, **41**, 14035-14037.

24 F. López Arbeloa, J. Bañuelos, V. Martinez, T. Arbeloa, I. López Arbeloa, *Int. Rev. Phys. Chem.*, 2005, **24**, 339-374.

25 T. A. Fayed, *Reviews in Fluorescence*, Chapter 4, Springer, 75-111, 2009

26 R. Sakamoto, S. Kusaka, Y. Kitagawa, M. Kishida, M. Hayashi, Y. Takara, M. Tsuchiya, J. Kakinuma, T. Takeda, K. Hirata, T. Ogino, K. Kawahara, T. Yagi, S. Ikehira, T. Nakamura, M. Isomura, M. Toyama, S. Ichikawa, M. Okumura, H. Nishihara, *Dalton Trans.*, 2012, **41**, 14035-14037.

27 C. Bronner, S. A. Baudron, M. W. Hosseini, C. A. Strassert, A. Guenet, L. De Cola, *Dalton Trans.*, 2010, **39**, 180–184.

28 S. R. Halper, M. R. Malachowski, H. M. Delaney, S. M. Cohen, *Inorg. Chem.*, 2004, **43**, 1242-1249.

29 G. Li, P. G. Bomben, K. C. D. Robson, S. I. Gorelsky, C. P. Berlinguette, M. Shatruk, *Chem. Comm.*, 2012, **48**, 8790-8792.

30 K. Hanson, A. Tamayo, V. V. Diev, M. T. Whited, P. I. Djurovich, M. E. Thompson, *Inorg. Chem.*, 2010, **49**, 6077–6084.

31 X. Liu, H. Nan, W. Sun, Q. Zhang, M. Zhan, L. Zou, Z. Xie, X. Li, C. Lu, Y. Cheng, *Dalton Trans.*, 2012, **41**, 10199-10210.

32 J. B. Paine, *The Porphyrins*, D. Dolphin, Academic Press: New York, 1978, Vol.1.

33 P. Bamfield, A. W. Johnson, J. Leng, *J. Chem. Soc.*, 1965, 7001-7005.

34 T. S. Teets, D. V. Partyka, A. J. Esswein, J. B. Updegraff, III, M. Zeller, A. D. Hunter, T. G. Gray, *Inorg. Chem. Comm.*, 2007, **46**, 6218-6220.

35 O. Moudam, in LCC-Toulouse, LCC Toulouse, 2007.

36 N. R. Kelly, S. Goetz, S. R. Batten and P. E. Kruger, *CrystEngComm*, 2008, **10**, 68-78.

37 Y. Takada, K. Nomura and S. Matsubara, *Org. Lett.*, 2010, **12**, 5204-5205.

38 V.-M. Mukkala and J. J. Kankare, *Helvetica Chimica Acta*, 1992, **75**, 1578-1592.

39 J. L. Sessler, L. R. Eller, W.-S. Cho, S. Nicolaou, A. Aguilar, J. T. Lee, V. M. Lynch, D. J. Magda, *Angew. Chem., Int. Ed.*, 2005, **44**, 5989-5992.

40 G. Ulrich, S. b. Goeb, A. De Nicola, P. Retailleau and R. Ziessel, *J. Org. Chem.*, 2011, **76**, 4489-4505.

41 J. M. Mellor, A. H. El-Sagheer, E-S. H. El-Tamany, R. N. Metwally, *Tetrahedron*, 2000, **56**, 10067-10074.

42 N. Zanatta, R. Barichello, H. G. Bonacorso, M. A. P. Martins, *Synthesis*, 1999, **5**, 765-768.

43 I. Noviandri, K. N. Brown, D. S. Fleming, P. T. Gulyas, P. A. Lay, A. F. Masters, L. Phillips, *J. Phys. Chem. B*, 1999, **103**, 6713-6722.

44 P. J. Hay, W. R. Wadt, *J. Chem. Phys.*, 1985, **82**, 270-283.

45 W. R. Wadt, P. J. Hay, *J. Chem. Phys.,* 1985, **82**, 284-298.

46 P. J. Hay, W. R. Wadt, *J. Chem. Phys.,* 1985, **82**, 299-310.

47 A. D. Becke, *J. Chem. Phys.,* 1993, **98**, 5648-5652.

48 Avogadro 1.1.0, http://sourceforge.net/projects/avogadro/

49 A. Hernandez Redondo, E. C. Constable, C. E. Housecroft, *Chimia*, 2009, **63**, 205.

50 E. C. Constable, C. E. Housecroft, P. Kopecky, E. Schönhofer and J. A. Zampese, *CrystEngComm*, 2011, **13**, 2742.

51 K. M. Smith, *Porphyrin and metalloporphyrin*, Elsevier Scientific Publishing: New York, 1975.

52 Y. Kajiwara, A. Nagai, Y. Chujo, *Bull. Chem. Soc. Jpn.,* 2011, **84**, 471-481.

53 G. Boschloo, E. A. Gibson, A. Hagfeldt, *J. Phys. Chem. Lett.,* 2011, **2**, 3016-3020.

54 G. F. Manbeck, W. W. Brennessel, R. Eisenberg, *Inorg. Chem.*, 2011, **50**, 3431-3441.